Article

Cell Reports

Cellular Heterogeneity in the Mouse Esophagus Implicates the Presence of a Nonquiescent Epithelial Stem Cell Population

Graphical Abstract

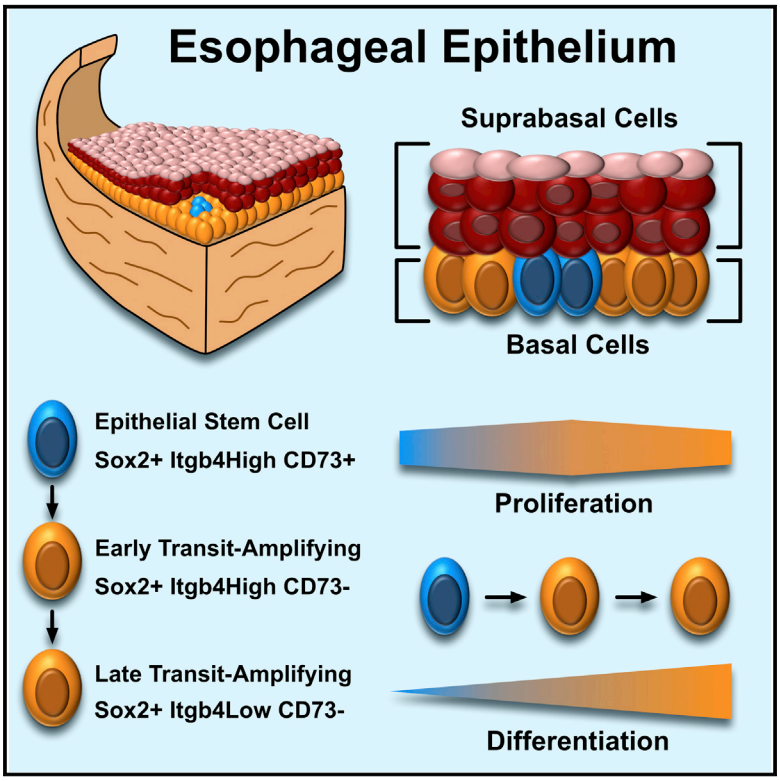

Highlights

3D esophageal organoids generated in vitro reflect in vivo tissue architecture

Cell-surface markers separate subpopulations of mouse esophageal basal epithelium

Subpopulations have distinct differentiation and proliferation properties

A nonquiescent stem cell population resides in the basal layer of the esophagus

Authors

Aaron D. DeWard, Julie Cramer, Eric Lagasse

Correspondence

lagasse@pitt.edu

In Brief

The esophageal epithelium is a rapidly renewing tissue, but conflicting reports have made it difficult to determine whether there is a separate stem cell population that contributes to cellular turnover. DeWard et al. now report heterogeneous cellular organization in the mouse esophagus, consisting of actively proliferating stem cells as well as more differentiated transit-amplifying cells.

DeWard et al., 2014, Cell Reports 9, 701–711
October 23, 2014
http://dx.doi.org/10.1016/j.celrep.2014.09.027

CellPress

Cell Reports
Article

Cellular Heterogeneity in the Mouse Esophagus Implicates the Presence of a Nonquiescent Epithelial Stem Cell Population

Aaron D. DeWard,[1,2] Julie Cramer,[1,2] and Eric Lagasse[1,2,*]
[1]Department of Pathology, University of Pittsburgh, Pittsburgh, PA 15219, USA
[2]McGowan Institute for Regenerative Medicine, University of Pittsburgh, Pittsburgh, PA 15219, USA
*Correspondence: lagasse@pitt.edu
http://dx.doi.org/10.1016/j.celrep.2014.09.027

SUMMARY

Because the esophageal epithelium lacks a defined stem cell niche, it is unclear whether all basal epithelial cells in the adult esophagus are functionally equivalent. In this study, we showed that basal cells in the mouse esophagus contained a heterogeneous population of epithelial cells, similar to other rapidly cycling tissues such as the intestine or skin. Using a combination of cell-surface markers, we separated primary esophageal tissue into distinct cell populations that harbored differences in stem cell potential. We also used an in vitro 3D organoid assay to demonstrate that Sox2, Wnt, and bone morphogenetic protein signaling regulate esophageal self-renewal. Finally, we labeled proliferating basal epithelial cells in vivo to show differing cell-cycle profiles and proliferation kinetics. Based on our results, we propose that a nonquiescent stem cell population resides in the basal epithelium of the mouse esophagus.

INTRODUCTION

The esophageal epithelium is a rapidly self-renewing tissue comprised of a basal cell layer and more differentiated suprabasal layers (Messier and Leblond, 1960). Proliferation is restricted to the basal cell layer, which contains cells that self-renew and differentiate over the lifespan of the tissue (Marques-Pereira and Leblond, 1965). To maintain tissue homeostasis, esophageal basal cells divide approximately twice per week to replace the differentiated cells that are shed into the lumen (Doupé et al., 2012). However, conflicting reports have made it difficult to determine if there is a separate subpopulation of slower-cycling stem cells that give rise to more differentiated cells in the basal layer, or if all basal cells represent a single progenitor population (Croagh et al., 2007; Doupé et al., 2012; Kalabis et al., 2008; Marques-Pereira and Leblond, 1965; Seery, 2002). In the intestine, multipotent LGR5$^+$ stem cells are found in readily identifiable structures called crypts and regenerate all epithelial lineages of the intestine (Barker et al., 2007). Conversely, the basal epithelium of the esophagus is morphologically more uniform and gives rise to a single cell lineage that forms the suprabasal layer. This simple structure has led to questions about the presence or necessity of a separate stem cell population in the basal epithelium, similar to the questions that have arisen regarding the interfollicular epidermis (Clayton et al., 2007; Doupé and Jones, 2013; Kaur and Potten, 2011; Lim et al., 2013; Mascré et al., 2012). Our results indicate that the basal epithelium of the mouse esophagus contains both proliferating stem and transit-amplifying cells.

RESULTS

Generation of 3D Esophageal Organoids

During development, both the Wnt and transforming growth factor β cell signaling pathways play an important role to properly form the adult esophagus as well as other endoderm-derived organs such as the trachea, stomach, and intestine (Barker et al., 2010; Jacobs et al., 2012; Que et al., 2006; van der Flier and Clevers, 2009). These signaling pathways were shown to control the intestinal stem cell niche in a 3D in vitro assay, in which intestinal stem cells generated organoids containing crypt structures (Sato et al., 2009, 2011). Related 3D assays have been used to characterize stem cells in the brain and breast, among other tissues (Maslov et al., 2004; Stingl et al., 2006). Therefore, we hypothesized that a similar assay could be applied to the esophagus. To test this, we removed the esophagus from mice and enzymatically dissociated the mucosa into single cells followed by suspension in Matrigel (Figures 1A–1C). We found that growth media supplemented with exogenous stem cell factors was required to generate 3D organoids (Figure 1D and Table S1). The organoids were morphologically similar to normal esophageal tissue after 9 days in culture, with small basal-like cells in contact with the extracellular matrix, large flat suprabasal-like cells in the interior, and hardened keratinized material in the center (Figures 1E and 1F). We then compared the cellular composition of the organoids to primary tissue using markers that are specific for the basal and more differentiated suprabasal cell layers (Figure 1G). The organoid outer cell layer was CK14$^+$, p63$^+$, and contained proliferating cells (incorporated EdU during a 2-hr incubation), similar to esophageal basal cells found in primary tissue. The organoid interior consisted of differentiated cells as shown by CK13$^+$ immunostaining, as well as abundant keratinization.

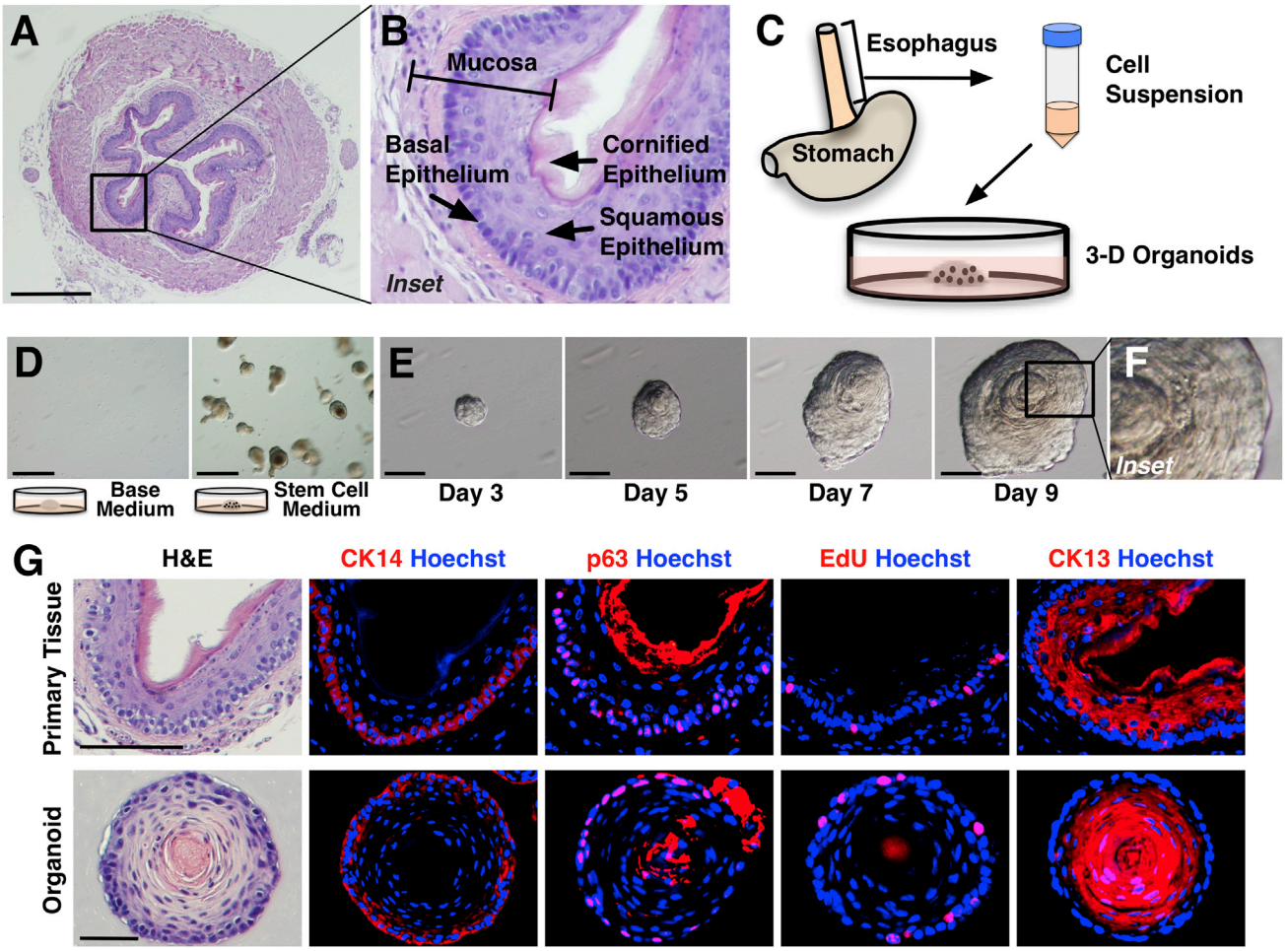

Figure 1. Primary Esophageal Cells Form 3D Organoids In Vitro

(A) Hematoxylin and eosin staining (H&E) of mouse esophagus cross-section. Scale bar represents 500 μm.

(B) Magnification of esophagus in (A).

(C) Isolation of primary esophageal cells to form organoids.

(D) Organoid assay in the absence and presence of growth factors. Scale bar represents 500 μm.

(E) Single organoid expanding over the course of 9 days. Scale bar represents 50 μm.

(F) Magnification of organoid captured on day 9.

(G) H&E and immunostaining (red) of cytokeratin 14 (CK14), p63, EdU, and cytokeratin 13 (CK13) for esophageal tissue sections (top) and sections of organoids generated in vitro (bottom). Sections were counterstained with Hoechst (blue). Scale bar represents 50 μm.

See also Figure S1 and Table S1.

Next, we determined if organoids were generated from single esophageal epithelial cells. Initially, we combined a single cell suspension of primary esophageal cells from GFP^+ and GFP^- mice. After organoids formed, they were always completely GFP^+ or GFP^-, indicating that they did not form by aggregation (Figures S1A and S1B). We then sorted primary esophageal cells with fluorescence-activated cell sorting (FACS) at the clonal level, and single cells were suspended in Matrigel to initiate organoid formation. After 9 days, organoids grew from a single cell with a similar morphology to those plated in a single cell suspension (Figure S1C).

We then assessed the role of Wnt and BMP signaling on esophageal organoid generation and self-renewal because these pathways govern esophageal development as well as the intestinal stem cell niche (Barker, 2014; Jacobs et al., 2012). Primary esophageal cells were suspended in Matrigel followed by the addition of complete stem cell medium, stem cell medium lacking Wnt agonists (Wnt3a/R-Spondin 2), or stem cell medium lacking the BMP inhibitor noggin. Organoids were generated with a similar efficiency under each condition, with a small decrease in organoid formation in the absence of noggin (Figure S1D). However, upon dissociation of organoids to single cells and replating, we found that exogenous noggin and Wnt agonists were required for self-renewal. On the other hand, organoids maintained in the presence of stem cell medium showed no decrease in self-renewal potential (passaged at least five times).

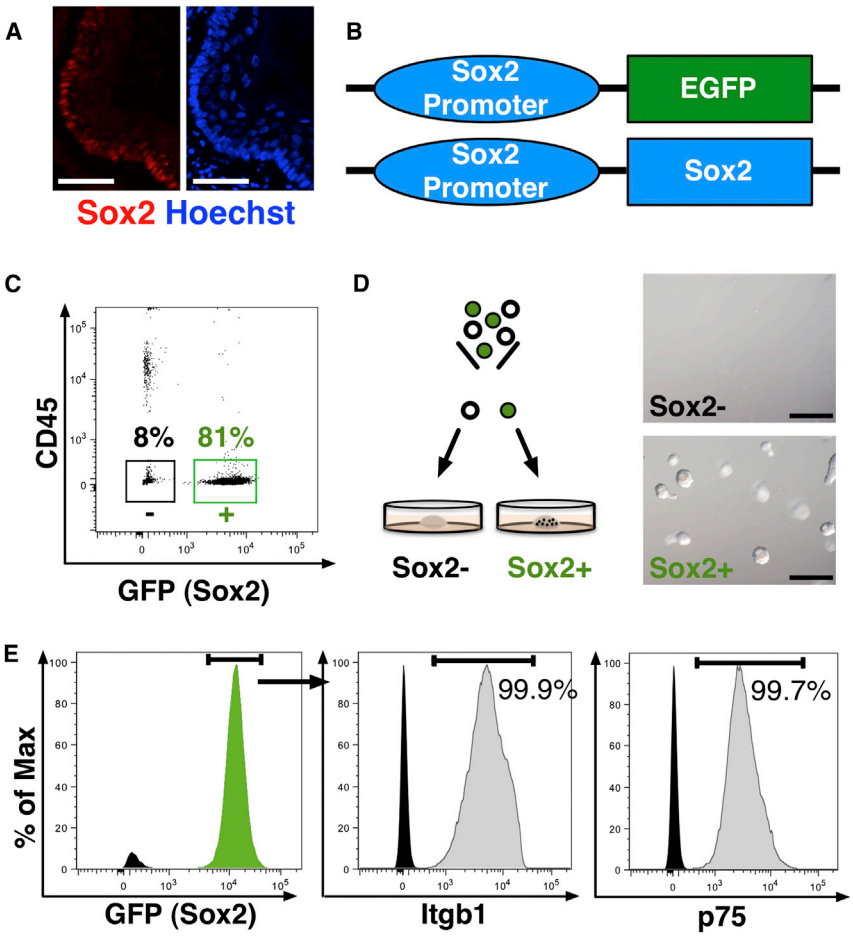

Figure 2. Sox2 Labels Esophageal Basal Epithelium

(A) Sox2 (red) immunostaining on primary esophageal tissue section counterstained with Hoechst (blue). Scale bar represents 50 μm.

(B) Mice with EGFP expression driven from the Sox2 promoter.

(C) Sox2$^+$ (gated in green) and Sox2- (gated in black) cell populations isolated from Sox2^{EGFP} mice. Percentages indicate the percent of total live cells.

(D) Sox2$^-$ and Sox2$^+$ cell populations sorted for in vitro organoid formation. Scale bar represents 500 μm.

(E) Histograms of Sox2$^+$ (GFP, green) cells gated and analyzed for β1 integrin (Itgb1) and p75 expression levels (shaded histograms). Percentages indicate the percent of positive expressing cells above unstained control cells (solid black histograms).

See also Figure S2.

Sox2 Marks Basal Epithelial Cells

We then asked whether the ability to generate organoids was restricted to basal epithelial cells, because these cells are thought to contain stem/progenitor cells (Messier and Leblond, 1960). Previous studies reported that Sox2 is constitutively expressed in all basal epithelial cells that give rise to Sox2-negative differentiated cells, which we confirmed by immunostaining (Figure 2A; Arnold et al., 2011; Liu et al., 2013). To separate primary live basal epithelial cells from other cells (i.e., hematopoietic, mesenchymal, or suprabasal), we used a genetic mouse model that had EGFP knocked in to one of the endogenous Sox2 alleles (Figure 2B). After isolating cells from the esophagus and separating the Sox2$^+$ and Sox2$^-$ cells by FACS, we found that only Sox2$^+$ cells generated organoids (Figures 2C, 2D, and S2A). We also found that the Sox2$^+$ population could be distinguished from the Sox2$^-$ population with the cell-surface marker EpCam, but EpCam expression is dim compared to that of GFP (Figure S2B). We confirmed that the Sox2$^+$ cell population was specific to basal cells, because all of the primary GFP$^+$ cells expressed the β1 integrin (Itgb1, CD29) and p75 (Figure 2E), which were previously used to separate esophageal basal cells (Doupé et al., 2012; Liu et al., 2013). Furthermore, we quantified the percent of EdU uptake in esophageal basal cells by both immunostaining and flow cytometry, and found no significant difference in the percent of EdU$^+$ cells when comparing the two methods (Figure S2C). Together, these data show that the sorted Sox2 GFP$^+$ population does not contain differentiated postmitotic suprabasal cells.

Sox2 Contributes to Organoid Formation and Self-Renewal

We next confirmed that Sox2$^+$ basal cells gave rise to differentiated cells using lineage tracing in the in vitro organoid assay. To label the Sox2$^+$ cells and their progeny, we used a tamoxifen inducible Sox2^{CreERT2} knockin mouse crossed with a mouse that contains a floxed stop signal to prevent EYFP expression (Figure 3A). Esophageal cells isolated from the Sox2$^{CreERT2/EYFP}$ mice were suspended in Matrigel to generate organoids followed by a 12 hr tamoxifen pulse to activate EYFP expression. After 9 days in culture, we found a majority of organoids with EYFP expression in all cells of the organoid, indicating that Sox2$^+$ cells generated the organoids (Figure 3B). However, treatment with 1 μM tamoxifen was not 100% efficient at labeling all cells (Figures S3A and S3B). We then generated Sox2$^{CreERT2/floxed}$ mice to genetically remove *Sox2* upon tamoxifen administration (Figure 3C). We confirmed the loss (~80%) of *Sox2* expression in organoids after the addition of tamoxifen using quantitative PCR analysis (Figure 3D). Previous studies showed that ablation of Sox2 expressing cells disrupted the esophageal basal epithelium (Arnold et al., 2011). Here, we found that genetically reducing *Sox2* expression resulted in an ~20% decrease in the total number of organoids formed in vitro (Figure 3E). We also found a significant decrease in the size of the organoids after *Sox2* deletion (Figure S3C). Upon organoid dissociation and passaging, we found that *Sox2* is required to generate new organoids (Figure 3F). Together, these data indicate that *Sox2* plays an important role in the generation and self-renewal of organoids, and Sox2$^+$ basal cells contain a stem cell population.

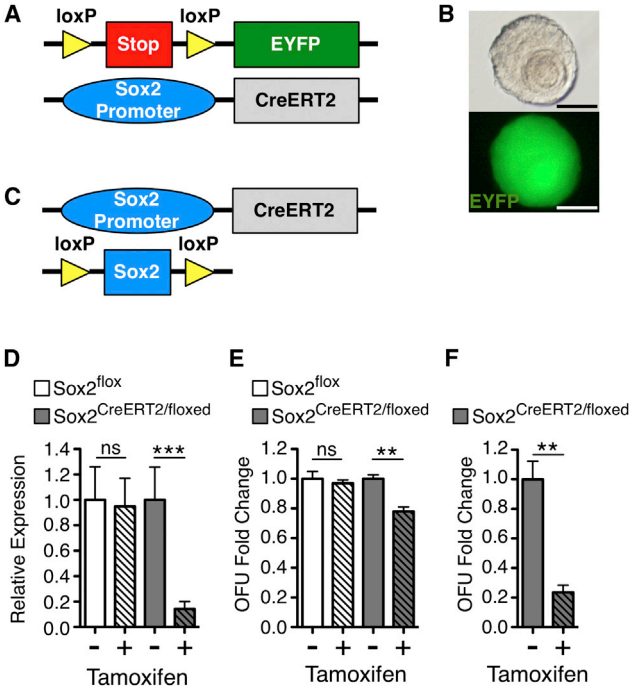

Figure 3. Expression of Sox2 Contributes to Organoid Formation and Self-Renewal

(A) $Sox2^{CreERT2/EYFP}$ mice express EYFP upon tamoxifen induced Cre expression from the Sox2 promoter.

(B) Organoid after 9 days in culture exposed to tamoxifen for the first 12 hr in culture. Scale bar represents 50 μm.

(C) $Sox2^{CreERT2/floxed}$ mice remove the remaining loxP flanked *Sox2* allele upon tamoxifen induced Cre expression from the *Sox2* promoter.

(D) Relative *Sox2* expression in tamoxifen treated versus untreated organoids derived from floxed *Sox2* mice ($Sox2^{flox}$) and $Sox2^{CreERT2/floxed}$ mice.

(E) Fold change in organoid-forming unit (OFU) frequency of primary esophageal cells isolated from $Sox2^{flox}$ and $Sox2^{CreERT2/floxed}$ mice in the presence or absence of tamoxifen.

(F) Fold change in OFU upon passaging the previously treated (+) or untreated (–) $Sox2^{CreERT2/floxed}$ derived organoids.

Data are represented as the mean ± SEM or ± SD for qPCR analysis. $^{**}p < 0.01$; $^{***}p < 0.001$; ns, not significant. See also Figure S3.

Identification of Cell-Surface Markers that Enrich for a Stem Cell Population

After establishing an in vitro assay to test for stemness and focusing on the basal cell compartment, we asked if stem cell heterogeneity could be observed among the basal cell population. Cell-surface proteins have been used to separate epithelial subpopulations to test for differences in stem cell potential (Croagh et al., 2007; Kaur et al., 2004). If all proliferating esophageal basal cells represent a single functionally equivalent cell population (Doupé et al., 2012), then we predict that separate cell populations would show similar stem cell characteristics. Using flow cytometry analysis, we found that esophageal basal cells ($Sox2^+$) express a range of low, medium, and high levels of α6 integrin (Itga6, CD49f) and β4 integrin (Itgb4, CD104), which form the integrin pair for laminin (Figure 4A). We also found heterogeneous expression of Itgb4 on basal cells by immunostaining (Figure 4B). We used FACS to separate primary esophageal basal cells based on their Itga6/Itgb4 expression. Limiting dilution analysis showed that the colony-forming unit frequency of cells expressing high levels of Itga6/Itgb4 was enriched 2.6-fold above the bulk population of basal cells (Figure 4C). In addition, the organoid-forming unit frequency of Itga6/$Itgb4^{High}$ cells was significantly higher than the Itga6/$Itgb4^{Low}$ and bulk cell populations (Figure 4D). These data show that Itga6/$Itgb4^{High}$ expressing basal cells enrich for cells that have stem cell features (i.e., increased colony-forming frequency and 3D organoid generation), similar to previous reports that correlated integrin expression with epithelial stemness (Adams and Watt, 1990; Croagh et al., 2007; Jones and Watt, 1993; Mascré et al., 2012). Previous work suggested that $CD34^+$ cells were candidate esophageal stem cells, but subsequent studies showed that epithelial cells do not express CD34 (Doupé et al., 2012; Kalabis et al., 2008). In our hands, CD34 appears to label an $EpCam^-$ stromal cell population of mesenchymal origin (Figure 4E).

Next, we asked whether the Itga6/$Itgb4^{High}$-expressing cells could be further enriched for stem cell activity. While screening the esophageal cells for mesenchymal cell-surface marker expression, we noticed that a subpopulation of Itga6/$Itgb4^{High}$ epithelial cells were $CD73^+$. We hypothesized that CD73 may be a stem cell marker for esophageal basal epithelial cells. We found $CD73^+$ basal cells by immunostaining, consistent with the predicted localization of an esophageal stem cell (Figure 5A). Using flow cytometry, the Itga6/$Itgb4^{High}$ population was separated into two populations, Itga6/$Itgb4^{High}CD73^+$ and Itga6/$Itgb4^{High}CD73^-$, and compared to the bulk population for the ability to generate organoids in vitro (Figure 5B). We found that the $CD73^+$ cell population had a significantly higher organoid-forming unit frequency compared to both the Itga6/$Itgb4^{High}CD73^-$ and the bulk cell populations (Figure 5C).

Our data are consistent with a hierarchical model, in which the Itga6/$Itgb4^{High}CD73^+$ population represents cells with the greatest stem cell potential followed by a continuum of increased differentiation (Figure 5D). To test this model further, we performed quantitative PCR analysis. We sorted primary esophageal basal cells based on their Itga6/Itgb4 and CD73 expression and assessed gene expression of cytokeratin 14 (*Krt14*), cytokeratin 13 (*Krt13*), cytokeratin 4 (*Krt4*), and involucrin (*Ivl*; Figure 5E). Each sorted cell population expressed the same levels of *Krt14* (basal cell marker), confirming that each population represents basal cells equally. On the other hand, we observed increased expression of the differentiating cell markers *Krt13* and *Krt4* as cells progress from the Itga6/$Itgb4^{High}CD73^+$ population, to the Itga6/$Itgb4^{High}CD73^-$ population, to the Itga6/$Itgb4^{Low}$ population. *Ivl*, a marker of differentiation in suprabasal cells, was below the threshold of detection in each population.

Characterization of Esophageal Organoids

Next, we determined whether esophageal organoids recapitulate the cell-surface heterogeneity observed on cells from primary tissue. Cells were isolated from mice and placed in Matrigel to generate organoids. After 9 days, organoids were collected and dissociated to single cells for subsequent analysis by flow cytometry (Figure S4A). Similar to primary tissue, we observed a range of Itga6 and Itgb4 expression. We found high CD73 expression on dissociated organoids in both the Itga6/$Itgb4^{High}$

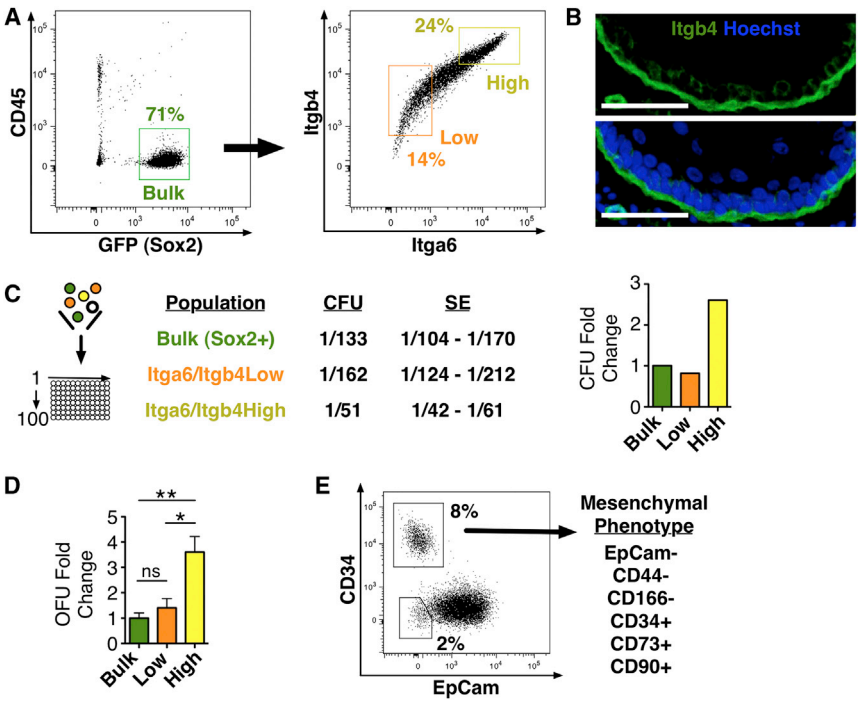

Figure 4. Cell-Surface Markers Enrich for Stem Cell Features

(A) Primary esophageal Sox2^{+} cells (green) isolated from Sox2^{EGFP} mice express low (orange) and high (yellow) Itga6 and Itgb4.

(B) Itgb4 immunostaining (green) of mouse esophagus counterstained with Hoechst (blue). Scale bar represents 50 μm.

(C) Schematic of limiting dilution analysis to sort primary cells ranging from 1 to 100 cells per well in a 96-well plate. The colony-forming unit (CFU) frequency and SE are indicated for each cell population sorted by FACS. Bar graph shows the CFU fold change compared to the bulk population for each sorted cell population.

(D) Fold change in OFU of the bulk, Itga6/Itgb4^{Low}, and Itga6/Itgb4^{High} populations after sorting primary esophageal cells and placing in the organoid assay.

(E) Flow cytometry plot of primary esophageal cells gated on EpCam^{-}CD34^{+} cells. CD34^{+} cells coexpress the mesenchymal markers CD73 and CD90, but do not express CD44 or CD166 (or Sox2).

Data are represented as the mean ± SEM. *$p < 0.05$; **$p < 0.01$; ns, not significant. Percentages indicate the percent of total live cells.

and Itga6/Itgb4^{Low} populations. However, the mean fluorescence intensity of CD73 was higher in the Itga6/Itgb4^{High} population compared to the Itga6/Itgb4^{Low} population, which is consistent with primary cells. These data show that organoids retain a similar cell-surface phenotype compared to cells isolated directly from primary tissue, with differences in overall expression levels once cells are cultured in vitro.

Organoids generated from primary esophageal epithelial cells can be passaged repeatedly in the presence of stem cell medium, indicating self-renewal potential (Figure S1D). We then asked if self-renewal potential was inherently lower in the Itga6/Itgb4^{Low} population, which represents a more differentiated cell population compared to the Itga6/Itgb4^{High} population. We sorted primary esophageal cells from the Itga6/Itgb4^{High} and Itga6/Itgb4^{Low} populations and generated organoids in stem cell medium. Organoids were dissociated to single cells and suspended in Matrigel to form new organoids. We found that organoids derived from both the Itga6/Itgb4^{High} and Itga6/Itgb4^{Low} populations were capable of self-renewal at a similar level, because they could be passaged repeatedly (Figure S4B). Even though fewer organoids were initially generated from the Itga6/Itgb4^{Low} population (Figure 4D), these data suggest that extrinsic factors (i.e., stem cell medium) are sufficient to maintain self-renewal potential once organoids are formed. Therefore, the total number of cell divisions (self-renewal potential) does not appear to be intrinsically defined by the current differentiation status of a given basal cell, similar to the regulation observed in proliferating intestinal epithelial cells (Ritsma et al., 2014).

Proliferation Kinetics of Esophageal Basal Epithelium

Although a quiescent long-term label-retaining epithelial cell may not be present in the basal layer (Doupé et al., 2012), we predict that an activated esophageal stem cell would undergo cell division less frequently than a transit-amplifying cell, whereas a fully differentiated cell of the suprabasal layer would not divide (Croagh et al., 2007; Potten and Loeffler, 1990). This is analogous to the proliferation kinetics observed in the intestine, where actively dividing LGR5^{+} cells give rise to the rapidly dividing transit-amplifying population, which eventually form the fully differentiated cell lineages of the intestine (Barker et al., 2007).

We examined the cell-cycle profile of the three basal epithelial cell populations that we identified (Figure 6A). Primary esophageal cells were isolated from mice and we found that the Itgb4^{High}CD73^{+} stem cell enriched population had fewer cells in G1 phase and significantly more cells in the S and G2/M phases compared to the Itgb4^{High}CD73- and Itgb4^{Low}CD73^{-} populations (Figures 6B and 6C). Next, we administered EdU to mice for 2, 12, or 24 hr and isolated cells from the esophagus. Short-term exposure to EdU (2 hr) resulted in a profile similar to the number of cells found in S phase (Figures 6D and 6E). After specifically examining EdU^{+} cells, we found that each of our identified cell populations were represented, indicating that each basal cell subpopulation remains actively dividing while having varying degrees of differentiation (Figure 6F). We also observed more EdU^{+} cells in the Itgb4^{High}CD73^{-} population compared to the Itgb4^{High}CD73^{+} population after 24 hr (Figure 6E), which suggested that the CD73^{-} population might serve as a faster dividing transit-amplifying cell population. Next, we examined the CD73^{-} population as a whole, irrespective of Itgb4 expression levels, and found that they incorporated a higher proportion of EdU over time compared to the Itgb4^{High}CD73^{+} population, in part because the CD73^{-} population represents the majority of basal cells (Figures S5A–S5C).

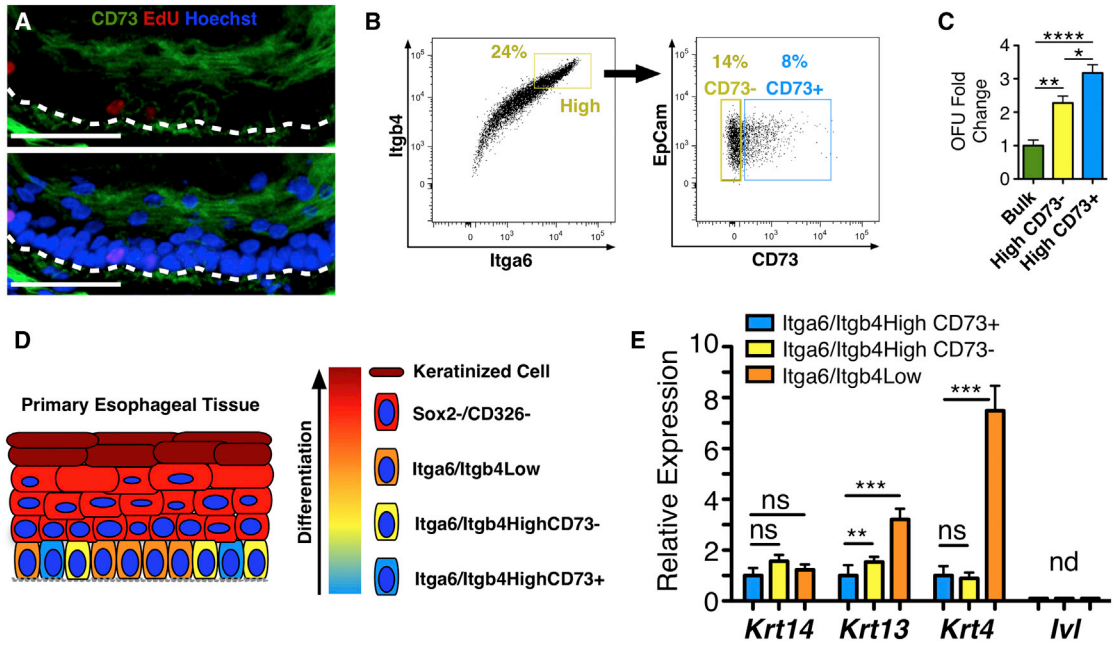

Figure 5. CD73 Labels Less-Differentiated Epithelial Basal Cells

(A) Esophageal tissue immunostained with CD73 (green), EdU (red, 2 hr exposure to EdU), and counterstained with Hoechst (blue). Dotted white line indicates basement membrane. Scale bar represents 50 μm.

(B) Gated Itga6/Itgb4^{High} population showing heterogeneous CD73^{+} (blue) and CD73^{-} (yellow) expression.

(C) Fold change in OFU of the bulk, Itga6/Itgb4^{High}CD73^{-}, and CD73^{+} cell populations after sorting primary esophageal cells and placing in organoid assay.

(D) Model of primary esophageal tissue showing continuum of stem cell potential/differentiation within the basal epithelial population.

(E) Quantitative PCR analysis showing relative expression levels of cytokeratin 14 (*Krt14*), cytokeratin 13 (*Krt13*), cytokeratin 4 (*Krt4*), and involucrin (*Ivl*). cDNA was generated after sorting Itga6/Itgb4^{High}CD73^{+} (blue), Itga6/Itgb4^{High}CD73^{-} (yellow), and Itga6/Itgb4^{Low} (orange) cells. Data were normalized to the Itga6/Itgb4^{High}CD73^{+} cell population. nd, expression levels under the threshold of detection.

Data are represented as the mean ± SEM or ± SD for qPCR analysis. *$p < 0.05$; **$p < 0.01$; ***$p < 0.001$; ****$p < 0.0001$; ns, not significant. Percentages indicate the percent of total live cells. See also Figure S4.

We then assessed the frequency of cell division to determine if distinct basal cell subpopulations do, in fact, proliferate at different rates. The stem-like Itgb4^{High}CD73^{+} cells divided approximately 1.4 times per week (± 0.1), whereas Itgb4^{High}CD73^{-} cells divided almost twice as fast at 2.3x per week (+/− 0.2), and Itgb4^{Low}CD73^{-} cells divided approximately 1.7 times per week (± 0.2; Figure 6G). We also determined that the entire CD73^{-} (i.e., the putative transit-amplifying) population divided more frequently (1.9 times per week ± 0.2) compared to the Itgb4^{High}CD73^{+} population (Figure S5D). In support of our proliferation analysis, we found that the bulk basal cell population divided 1.7 times per week (± 0.2; Figure 6G), similar to previously reported proliferation kinetics (1.9 times per week ± 0.1) that characterized the total basal cell population (Doupé et al., 2012).

Next, we characterized esophageal basal cells at the clonal level in vitro. Single GFP^{+} primary esophageal cells were sorted from the Itgb4^{High}CD73^{+} and Itgb4^{High}CD73^{-} populations and six separate clones were expanded from each population. Consistent with our observed proliferation rates, we found a higher total number of cells when the original cell was from the faster dividing Itgb4^{High}CD73^{-} population (Figure 6H). We also found that clones derived from the Itgb4^{High}CD73^{+} population generated organoids more efficiently (Figure 6I), similar to our results when cells were sorted directly from primary tissue (Figure 5C).

Challenge with Retinoic Acid Alters the Epithelial Basal Cell Populations

We then asked whether challenge with all-*trans* retinoic acid (atRA), known to promote a stress response in esophageal epithelium by inducing differentiation (Chang et al., 2007; Doupé et al., 2012), alters the different basal cell populations we identified. Mice were exposed to atRA for 5 days and analyzed on day 6 (Figure 7A). In agreement with others (Doupé et al., 2012), we observed a significant increase in the percent of Ki67^{+} esophageal basal cells as well as upregulation of cellular retinoic acid-binding protein 2 (CRABP2) upon exposure to atRA (Figures 7B and 7C). Next, we used flow cytometry to determine the percent of Itga6/Itgb4^{High}CD73^{+}, Itga6/Itgb4^{High}CD73^{-}, and Itga6/Itgb4^{Low} cells that comprise the basal epithelium in treated versus untreated mice. We found a decrease in the percent of Itga6/Itgb4^{High}CD73^{+} and Itga6/Itgb4^{High}CD73^{-} cells, and a significant increase in the percent of Itga6/Itgb4^{Low} cells (Figure 7D). This shows that atRA induced a shift in the esophageal basal epithelium toward the more differentiated Itga6/Itgb4^{Low} cell population in vivo.

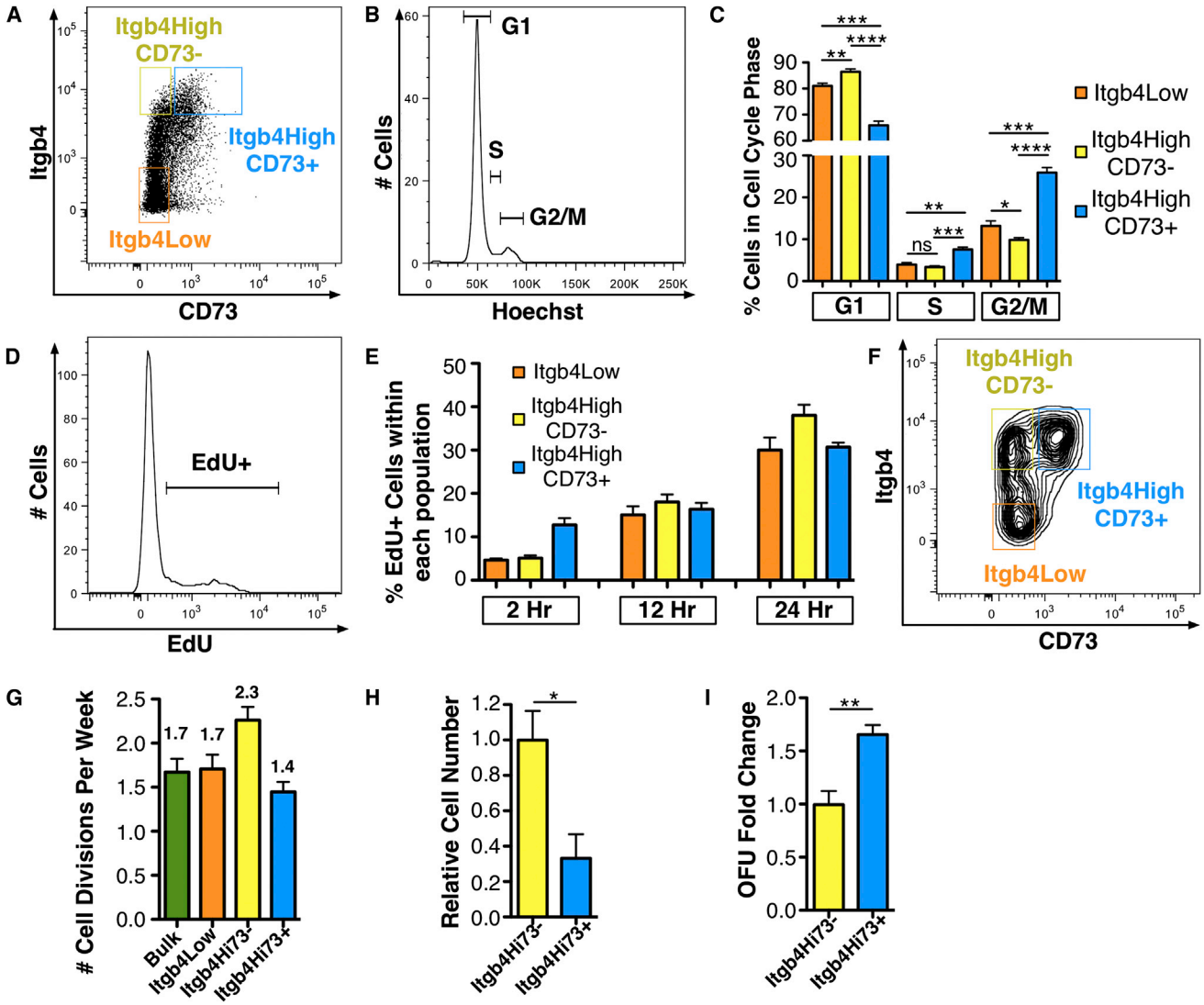

Figure 6. Cell-Cycle and Proliferation Kinetics of Esophageal Basal Epithelial Cells

(A) Three separate cell populations in primary esophageal basal epithelium: Itgb4^{High}CD73^{+} (blue), Itgb4^{High}CD73^{-} (yellow), and Itgb4^{Low} (orange).

(B) Representative gating strategy to determine the percent of cells in G1, S, or G2/M cell-cycle phases from each of the three cell populations in (A).

(C) The percent of cells in G1, S, or G2/M.

(D) Representative gating strategy to determine the percent of primary esophageal cells that incorporated EdU.

(E) The percent of EdU incorporation in esophageal basal epithelial cells after exposing mice to EdU for 2, 12, or 24 hr.

(F) Each of the cell populations defined in (A) are evident in the contour plots after first gating on EdU^{+} (2 hr exposure) proliferating basal cells.

(G) Approximate frequencies of cell division (number of cell divisions per week) for each of the cell populations outlined in (A) as well as the bulk (EpCam^{+}) cell population.

(H) Relative total number of cells generated from one single Itgb4^{High}CD73^{+} or Itgb4^{High}CD73^{-} cell after clonal expansion in vitro. Data were derived from six separate clones for each population.

(I) OFU fold change of expanded clones generated from single Itgb4^{High}CD73^{-} cells (three separate clones tested) and single Itgb4^{High}CD73^{+} cells (two separate clones tested).

Data are represented as the mean ± SEM. For each EdU time point, n = 4 or 5 mice, n = 5 mice for cell-cycle analysis. *p < 0.05; **p < 0.01; ***p < 0.001; ****p < 0.0001; ns, not significant. See also Figure S5.

DISCUSSION

Our results indicate the presence of a stem cell population in the esophageal epithelium. This population represents a small fraction of basal cells that are functioning as less differentiated nonquiescent stem cells, whereas a majority of basal cells are serving as faster dividing transit-amplifying cells. We identified cell-surface markers that distinguish the stem and transit-amplifying populations, with each basal cell likely falling somewhere along a continuum of proliferation and differentiation

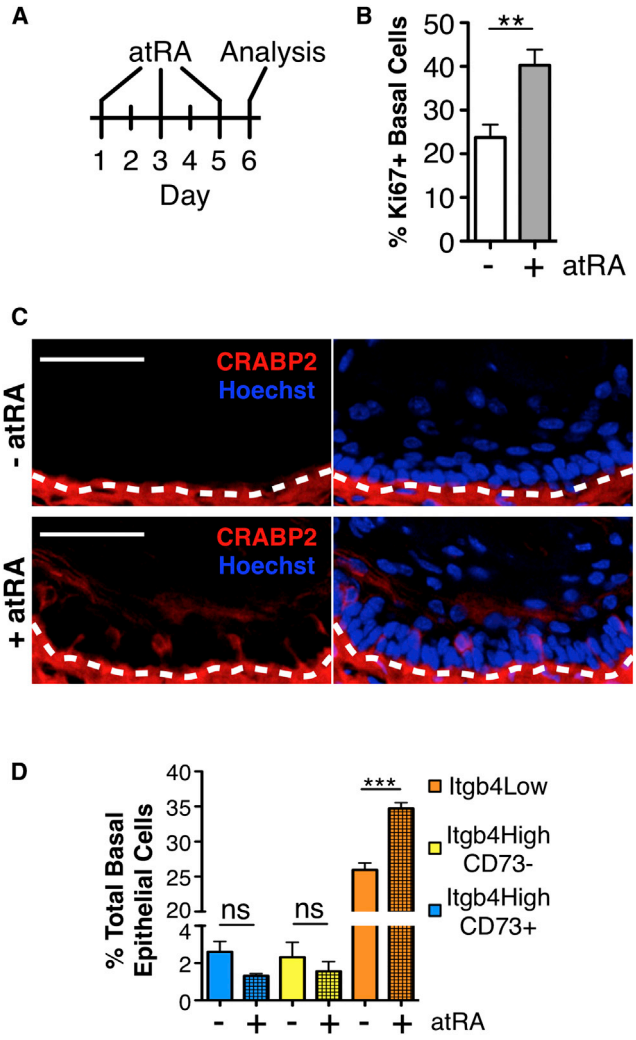

Figure 7. Retinoic Acid Increases the Number of Differentiated Basal Cells in Mice

(A) All-*trans* retinoic acid (atRA) was injected in mice on days 1, 3, and 5. Mice were analyzed on day 6 (n = 5 mice).

(B) Percent of Ki67$^+$ basal cells in mice treated with (shaded bar) or without (open bar) atRA. Ki67$^+$ cells were analyzed by immunostaining eight different sections (n = 3 mice).

(C) CRABP2 (red) immunostaining of esophageal tissue from mice treated (bottom) or untreated (top) with atRA. Sections were counterstained with Hoechst (blue). White dotted line indicates basement membrane. Scale bar represents 50 μm.

(D) The percent of total basal epithelial cells comprised of the Itgb4^{High}CD73$^+$ (blue), Itgb4^{High}CD73$^-$ (yellow), and Itgb4^{Low} (orange) cell populations in mice treated with atRA compared to untreated control mice (n = 5 mice).

Data are represented as the mean ± SEM. **p < 0.01; ***p < 0.001.

(Potten and Loeffler, 1990). At one end of the spectrum, the Itgb4^{High}CD73$^+$ cells have the greatest stem cell potential, whereas CD73$^-$ transit-amplifying cells range in levels of maturation (e.g., from early transit-amplifying to more differentiated late transit-amplifying). This shows that proliferating esophageal basal cells may not necessarily represent a single functionally equivalent population of cells dividing at the same rate, despite their putative stochastic cell fate behavior (Doupé et al., 2012). The different conclusions can be attributed to the experimental methods used among groups. Jones and colleagues used an inducible Ah$^{CreERT/EYFP}$ reporter mouse to randomly label esophageal basal epithelium. Some of the labeled clones might have originated from a CD73$^+$ stem cell and others might have originated from CD73$^-$ transit-amplifying cells. Without defined promoters to label specific subpopulations or knowing the location of a stem cell niche, it is difficult to distinguish the differentiation status of the initial labeled cell. Therefore, many of the long-term clones could have been derived from labeled CD73$^+$ stem cells. Ultimately, the longevity of each clone was due to balanced but randomly defined symmetric or asymmetric cell divisions. The authors did not find any discernable differences in the proliferation and differentiation of single cell derived clones under homeostatic conditions, which fit the overall concept of a single progenitor model. Conversely, our studies used cell-surface markers to prospectively isolate distinct cell populations within the total esophageal basal epithelium. This allowed us to determine key differences in proliferation and differentiation by comparing each population, which would not have been possible if we only examined the bulk cell population.

Because of the morphological similarities between esophageal and skin epithelium, it is interesting to consider the parallels regarding the stem cell compartment in both of these tissues. Recent work from Blanpain and colleagues used two separate promoters, cytokeratin 14 and involucrin, to trace distinct cell populations in the skin basal epithelium and found different contributions of stem and progenitor cells to epidermal maintenance (Mascré et al., 2012). This result contrasted with studies that used a single Ah$^{CreERT/EYFP}$ reporter mouse to label skin epithelium, in which the authors suggested all basal epithelial cells of the skin have equal stem cell potential (Clayton et al., 2007).

No discernable epithelial stem cell niche has been previously identified in the esophagus, which has led to the assumption that the entire basal cell layer constitutes a progenitor cell niche (Doupé and Jones, 2013). A key difference between the esophagus and the intestine is thought to be the restricted niche space in the intestine (Doupé and Jones, 2013). The intestinal stem cell niche provides external signals (e.g., Wnt and noggin) to maintain stemness at the base of the crypt (Barker, 2014; Barker et al., 2007). The Wnt and noggin/BMP pathways are also essential regulators of epithelial morphogenesis during esophageal development, when the esophagus and trachea separate to form their respective tissues (Jacobs et al., 2012). Our data suggest that these signals persist in adult esophageal tissue to maintain stemness and permit self-renewal. This raises the question then, if there is a stem cell niche in the esophagus that is mechanistically related to the intestine, in which esophageal basal cell stemness is maintained or lost based on competition and cellular proximity to extracellular "niche" signals (Ritsma et al., 2014; Snippert et al., 2010; Walther and Graham, 2014). Another possibility is that Wnt signals are derived from basal epithelial cells themselves, similar to the autocrine mechanism identified in a population of interfollicular epidermal stem cells (Lim et al., 2013). Either way, our in vitro data suggest that extracellular signals play an essential role to maintain

stemness, because exogenous Wnt/noggin was required for organoid self-renewal.

Whereas basal cells appeared to be hierarchically organized (i.e., stem cells differentiated into transit-amplifying cells), future work will require an examination of cell fate at the clonal level in vivo within each cell population. Using our experimental approach, we were unable to discern symmetric versus asymmetric cell fate decisions or determine whether certain basal populations adhere to a model of population asymmetry (Watt and Hogan, 2000). These studies will entail lineage tracing and quantitative analysis of single cell derived clones using promoters specific to both the $CD73^{+}$ stem cell and $CD73^{-}$ transit-amplifying populations. Jones and colleagues previously showed that bulk esophageal homeostasis is maintained by stochastic population renewal as opposed to defined asymmetric cell divisions, and concluded that a separate stem cell population does not reside in the basal epithelium (Doupé et al., 2012). These data, along with the absence of a specialized stem cell niche in the esophagus, were a major reason that all basal cells were defined as a single progenitor cell population (Doupé and Jones, 2013). In the intestine, stem cells also self-renew via population asymmetry, but all proliferating intestinal epithelial cells are not considered a single "progenitor" population because stem cells reside in and compete for niche space (Lopez-Garcia et al., 2010; Ritsma et al., 2014; Walther and Graham, 2014).

Our data do not conflict with the notion of esophageal stem cells undergoing population renewal, but they do suggest that there is a separate stem cell population with the following attributes: (1) esophageal stem cells cycle slower/less often than transit-amplifying cells, but are not quiescent; (2) esophageal stem cells are the least differentiated epithelial cell population in the esophagus; (3) esophageal stem cells have self-renewal potential and generate differentiated cell phenotypes in vitro; and (4) esophageal stem cells require extrinsic "niche" signals to self-renew, whereas transit-amplifying cells have the plasticity to behave like less differentiated stem cells given the right external cues. Each of these attributes could also be used to describe intestinal stem cells, yet there is general agreement that the intestine is comprised of both stem and transit-amplifying cell populations. Therefore, we propose a model for the esophageal basal epithelium that consists of separate populations of proliferating stem cells and more differentiated transit-amplifying cells.

Our findings have important implications for tissue repair and disease. Stem or more differentiated cells might make separate contributions to tissue repair after injury. In addition, basal epithelial cells likely act as the cells of origin for squamous cell carcinoma (Liu et al., 2013), but the distinct contribution of stem cells versus more differentiated cells will be important to determine. A recent study found that inhibition of differentiation in esophageal basal cells led to an expansion of clones that expressed increased Itgb4 at the transcript and protein levels (Alcolea et al., 2014). Using our model as a guide, these data point to an expansion of the less differentiated $Itgb4^{High}$, and possibly $CD73^{+}$ stem cell population, when normal differentiation is disrupted. Finally, a prominent but controversial hypothesis suggests that normal esophageal stem cells may be the cell of origin for Barrett's metaplasia. Our studies are an important step forward to now capably test this long-standing hypothesis.

EXPERIMENTAL PROCEDURES

Mice

The following strains of mice were purchased from Jackson Laboratories and used in this study: wild-type C57BL/6 (#000664), transgenic EGFP C57BL/6 (#004353), mixed 129S C57BL/6 knockin mice expressing EGFP from the Sox2 promoter ($Sox2^{EGFP}$; #017592), mixed 129S C57BL/6 knockin mice expressing tamoxifen-inducible Cre from the Sox2 promoter ($Sox2^{CreERT2}$; #017593), C57BL/6 transgenic loxP-stop-loxP EYFP (#006148), and mixed 129S C57BL/6 floxed Sox2 mice ($Sox2^{flox}$; #013093). Mice were bred and housed in the Division of Laboratory Animal Resources facility at the University of Pittsburgh McGowan Institute for Regenerative Medicine. Experimental protocols followed NIH guidelines for animal care and were approved by the Institutional Animal Care and Use Committee at the University of Pittsburgh.

Esophageal Tissue Isolation

The esophagus was removed from mice and the mucosa was physically separated from the submucosa using forceps and chopped into small pieces with a straight edge razor. Cells were dissociated by incubating at 37°C in 1× Trypsin-EDTA for 60 min, vortexing every 15 min. Culture medium (Dulbecco's modified Eagle's medium/F12) was added to inactivate the trypsin. Remaining tissue clumps were removed by passing the cells through a 70 μm sterile filter. For cell-sorting experiments, the mucosa was isolated from at least four mice and pooled to obtain a sufficient number of cells.

Immunofluorescence

Tissue was fixed in 4% paraformaldehyde for 4 hr, and stored in 1× PBS followed by imbedding in paraffin, or stored in 30% sucrose for 12 hr and then embedded in optimal cutting temperature medium, and frozen and stored at −80°C. Tissue sections were mounted on glass slides. Sections were washed with PBS and blocked with 5% BSA for 30 min. Sections were then incubated in primary antibody for at least 1 hr and secondary antibody for 1 hr. Sections were mounted with Hoechst mounting media. Images were captured with an Olympus IX71 inverted microscope.

Generation of 3D Organoids

Primary esophageal cells (500–5,000 cells, depending on the experiment) were suspended in 50 μl Matrigel (BD Biosciences) on ice. The Matrigel-containing cells were placed as a droplet in a 24-well tissue culture plate followed by incubation at 37°C for 30 min to allow solidification of the gel. Growth medium was added to cover the Matrigel and incubated at 37°C to allow organoid formation. Growth medium consisted of Advanced Dulbecco's modified Eagle's medium/F12, 1× N2, and 1× B27 Supplements, 1× Glutamax (Life Technologies), 1× HEPES, 1× penicillin/streptomycin (Mediatech), 1 mM N-acetyl-L-cysteine, 100 μM gastrin, 10 mM nicotinamide, 10 μM SB202190 (Sigma), 50 ng/ml epidermal growth factor, 100 ng/ml Noggin (Peprotech), 100 ng/ml Wnt3A, 100 ng/ml R-Spondin 2 (R&D), and 500 nM A8301 (Tocris; Table S1). Media were changed twice over the 9-day length of the experiment.

Antibodies and Reagents

Antibodies specific to the following antigens were purchased for immunofluorescence from Abcam: Cytokeratin 14 (#ab7800), p63 (#ab53039), Cytokeratin 13 (#ab92551), Sox2 (#ab97959), and Ki67 (#ab15580). From BD Biosciences: CD104 (Itgb4, #553745), CRABP2 (#560234), and CD73 (#550738). The following reagents were used for fluorescence analysis from Life Technologies: Hoechst (#H21492) and Click-iT Alexa Fluor 594 EdU labeling kit (#C10339). Antibodies specific to the following antigens were purchased for flow cytometric analysis from BD Biosciences: PerCP-Cy5.5 CD45 (#550994, 1:50), PE-Cy7 CD45 (#552848, 1:50), APC CD45 (#559864, 1:50), PE-Cy7 Streptavidin (#557598, 1:50), PE CD73 (#550741, 1:25), FITC CD34 (#553733, 1:25), PE CD90 (1:50), and PE CD44 (#553134, 1:25). From Biolegend: Biotin CD104 (Itgb4, #123604, 1:50), APC CD49f (Itga6, #313616, 1:50), APC-Cy7 CD326

(EpCam, #118217, 1:25), and APC CD29 (Itgb1, #102215, 1:50). From eBioscience: PE CD166 (#12-1661, 1:25). From Abcam: p75 (#ab8874, 1:50). The following reagents were used for flow cytometric staining from Life Technologies: Hoechst (#H21492), Sytox Blue (#S34857), and Click-iT Alexa Fluor 647 EdU labeling kit (#C10424). atRA was purchased from Sigma and tamoxifen was from EMD Millipore.

Flow Cytometry

Cell suspensions were stained with antibodies on ice in the dark for 1 hr. Two milliliters of flow buffer (2% FBS in Hank's balanced salt solution) was added to tubes, and mixed and centrifuged at 400 × *g* for 5 min. The supernatant was aspirated, secondary antibody was added if necessary, and reactions were incubated in the dark on ice for 1 hr. Cells were rinsed and spun again as described. The final cell pellet was suspended in 400 μl of flow buffer containing a 1:600 dilution of Sytox Blue viability stain. Cells were acquired using a BD Aria II Cell Sorter or a Miltenyi MACSQuant, and postacquisition analysis was performed using FlowJo software.

Tamoxifen Induction

Tamoxifen (10–1,000 nM) was added to the organoid-forming stem cell medium to initiate Cre expression in cells cultured in vitro. After 12 hr, the medium was removed and fresh medium without tamoxifen was added to the cultures for the remainder of the experiment. Organoid formation was assessed after 9 days in culture.

Cell Division Frequency

The frequency of cell division was determined using the equation: $T_{div} = T_{chase}/((EdU\%/100\%) - f_s)$, where T_{div} represents how often a cell divides, T_{chase} represents the amount of time that the cells are exposed to continuous EdU incorporation, *EdU%* is the percent of cells that have incorporated EdU, and f_s represents the percent of cells in S phase at the time of EdU labeling. A similar method was used to identify proliferation rates in subpopulations of basal skin epithelium (Mascré et al., 2012). Data from individual mice exposed to EdU for 12 hr (n = 4 mice) and 24 hr (n = 5 mice) were used to determine the average frequency of cell division.

Proliferation Assay and Cell-Cycle Analysis

Proliferation was assessed by injecting 100 μg EdU into mice intraperitoneally followed by flow cytometry analysis. For the 2 hr and 12 hr time points, EdU was injected at time 0 and mice were killed after 2 or 12 hr. For the 24-hr time point, EdU was injected at time 0 and again after 12 hr. Cells were then isolated from the esophagus and stained with the appropriate antibodies. EdU was detected by flow cytometry using the Click-iT Alexa Fluor 647 EdU labeling kit. Data were obtained from individual mice (n = 4 or n = 5). For cell-cycle analysis, primary esophageal cells were isolated from mice (n = 5) and stained with Hoechst as well as the indicated antibodies. The percent of cells in each cell-cycle phase was determined by gating on histograms showing DNA content (Hoechst) in a linear scale.

Colony-Forming Unit Frequency

Limiting dilution analyses were performed by sorting a range of primary GFP^+ esophageal cells (ranging from 1 up to 100 cells per well) into respective rows of 96-well plates seeded with irradiated LA7 feeder cells. Colonies were scored after 2–3 weeks postplating (positive wells contained GFP^+ cells) and candidate stem cell frequencies with SE of sorted subpopulations were determined with L-Calc (StemCell Technologies).

Organoid-Forming Unit Frequency

Equal numbers of primary esophageal cells were suspended in Matrigel to form organoids. After 9 days, organoids (spheres greater than 50 μm) were counted. Organoid-forming unit (OFU) frequency was determined by dividing the number of organoids by the number of cells placed in Matrigel. Fold change was determined by comparing OFU from specific subpopulations to the OFU from the bulk cell population ($Sox2^+$ or $EpCam^+$).

Organoid Collection and Passaging

Organoids were removed from Matrigel upon incubation with a dispase solution. Dispase solution consisted of 0.2% dispase I (Life Technologies), 0.1% collagenase type II (MP Biomedicals), and 20 μg/ml DNase I (Roche) in 1× HBSS containing 1% HEPES buffer. Matrigel was digested in dispase solution at 37°C for 15 min. Organoids were washed with 1× PBS and centrifuged at 200 × *g* for 3 min. Organoids were resuspended in 1× trypsin-EDTA and incubated at 37°C for 45 min to dissociate cells. Cells were washed and analyzed by flow cytometry or suspended in Matrigel to generate new organoids.

Quantitative PCR Analysis

Organoids grown in Matrigel were lysed and RNA was isolated using the RNeasy kit (QIAGEN). RNA was quantified with the Nanodrop 2000c Spectrophotometer (Thermo Scientific). Reverse transcription was performed using iScript RT Supermix (Bio-Rad) followed by real-time PCR on an ABI StepOne Plus Real-Time PCR machine (Applied Biosystems). For FACS-sorted cell populations, cDNA was generated using the Cells-to-cDNA II kit (Life Technologies). TaqMan probes and primers were purchased from Life Technologies (Table S2). Expression was normalized to *Gapdh*. Error bars represent upper and lower error limits based on replicate variability.

Clonal Cell Expansion In Vitro

Esophageal tissue was collected from GFP^+ mice and digested to single cells. FACS was used to sort one cell per well in multiple 96-well plates seeded with irradiated LA7 feeder cells. Single cells were sorted from either the Itga6/Itgb4-^{High} or Itga6/$Itgb4^{Low}$ cell populations. After 14 days, wells containing a GFP^+ colony were treated with trypsin to remove the cells from the plate. All cells were subsequently placed in 12-well plates seeded with irradiated LA7 cells. After 14 days, cells were again removed and all cells were placed in six-well plates seeded with irradiated LA7 cells. Six separate clones were generated from each original cell population. After another 14 days, cells were removed from the plates and the total number of GFP^+ cells was determined for each clone. The OFU frequency was assessed for several clones by suspending the cells in Matrigel in the presence of stem cell medium.

Challenge with Retinoic Acid

Five mice were given intraperitoneal injections of 400 μg atRA on days 1, 3, and 5. Esophageal tissue was collected from mice on day 6 for subsequent analysis and compared to control mice (n = 5). A portion of tissue was fixed and stained with Ki67 or CRABP2 to confirm the response to atRA. The remaining tissue was digested to single cells and analyzed by flow cytometry. The number of cells within each of the three gated populations ($Itgb4^{High}CD73^+$, $Itgb4^{High}CD73^-$, and $Itgb4^{Low}$) was used to determine the percent of total basal epithelial cells comprised by the three different populations.

Statistical Analysis

Statistical significance was determined with two-tailed Student's t test (Figures 3D–3F, 4D, 5C, 5E, 6C, 6H, 6I, 7B, 7D, S1D, S2C, S3C, and S5D).

SUPPLEMENTAL INFORMATION

Supplemental Information includes five figures and two tables and can be found with this article online at http://dx.doi.org/10.1016/j.celrep.2014.09.027.

AUTHOR CONTRIBUTIONS

A.D.D. designed and performed experiments, analyzed data, and wrote the manuscript; J.C. performed qPCR and edited the manuscript; and E.L. supervised the project and edited the manuscript.

ACKNOWLEDGMENTS

The authors acknowledge Lynda Guzik for operation and technical assistance with cell sorting experiments, and Andrew Bell for assistance with immunostaining. This work was supported by funds from the Commonwealth of Pennsylvania (to A.D.D., J.C., and E.L.), NIH grant R01 DK08571 (to A.D.D., J.C.,

and E.L.), the University of Pittsburgh McGowan Institute for Regenerative Medicine (to A.D.D., J.C., and E.L.), and the Department of Pathology Post-doctoral Research Training Program (to A.D.D.).

Received: January 19, 2014
Revised: August 15, 2014
Accepted: September 15, 2014
Published: October 16, 2014

REFERENCES

Adams, J.C., and Watt, F.M. (1990). Changes in keratinocyte adhesion during terminal differentiation: reduction in fibronectin binding precedes alpha 5 beta 1 integrin loss from the cell surface. Cell *63*, 425–435.

Alcolea, M.P., Greulich, P., Wabik, A., Frede, J., Simons, B.D., and Jones, P.H. (2014). Differentiation imbalance in single oesophageal progenitor cells causes clonal immortalization and field change. Nat. Cell Biol. *16*, 615–622.

Arnold, K., Sarkar, A., Yram, M.A., Polo, J.M., Bronson, R., Sengupta, S., Seandel, M., Geijsen, N., and Hochedlinger, K. (2011). Sox2(+) adult stem and progenitor cells are important for tissue regeneration and survival of mice. Cell Stem Cell *9*, 317–329.

Barker, N. (2014). Adult intestinal stem cells: critical drivers of epithelial homeostasis and regeneration. Nat. Rev. Mol. Cell Biol. *15*, 19–33.

Barker, N., van Es, J.H., Kuipers, J., Kujala, P., van den Born, M., Cozijnsen, M., Haegebarth, A., Korving, J., Begthel, H., Peters, P.J., and Clevers, H. (2007). Identification of stem cells in small intestine and colon by marker gene Lgr5. Nature *449*, 1003–1007.

Barker, N., Huch, M., Kujala, P., van de Wetering, M., Snippert, H.J., van Es, J.H., Sato, T., Stange, D.E., Begthel, H., van den Born, M., et al. (2010). Lgr5(+ve) stem cells drive self-renewal in the stomach and build long-lived gastric units in vitro. Cell Stem Cell *6*, 25–36.

Chang, C.L., Lao-Sirieix, P., Save, V., De La Cueva Mendez, G., Laskey, R., and Fitzgerald, R.C. (2007). Retinoic acid-induced glandular differentiation of the oesophagus. Gut *56*, 906–917.

Clayton, E., Doupé, D.P., Klein, A.M., Winton, D.J., Simons, B.D., and Jones, P.H. (2007). A single type of progenitor cell maintains normal epidermis. Nature *446*, 185–189.

Croagh, D., Phillips, W.A., Redvers, R., Thomas, R.J., and Kaur, P. (2007). Identification of candidate murine esophageal stem cells using a combination of cell kinetic studies and cell surface markers. Stem Cells *25*, 313–318.

Doupé, D.P., and Jones, P.H. (2013). Cycling progenitors maintain epithelia while diverse cell types contribute to repair. BioEssays *35*, 443–451.

Doupé, D.P., Alcolea, M.P., Roshan, A., Zhang, G., Klein, A.M., Simons, B.D., and Jones, P.H. (2012). A single progenitor population switches behavior to maintain and repair esophageal epithelium. Science *337*, 1091–1093.

Jacobs, I.J., Ku, W.Y., and Que, J. (2012). Genetic and cellular mechanisms regulating anterior foregut and esophageal development. Dev. Biol. *369*, 54–64.

Jones, P.H., and Watt, F.M. (1993). Separation of human epidermal stem cells from transit amplifying cells on the basis of differences in integrin function and expression. Cell *73*, 713–724.

Kalabis, J., Oyama, K., Okawa, T., Nakagawa, H., Michaylira, C.Z., Stairs, D.B., Figueiredo, J.L., Mahmood, U., Diehl, J.A., Herlyn, M., and Rustgi, A.K. (2008). A subpopulation of mouse esophageal basal cells has properties of stem cells with the capacity for self-renewal and lineage specification. J. Clin. Invest. *118*, 3860–3869.

Kaur, P., and Potten, C.S. (2011). The interfollicular epidermal stem cell saga: sensationalism versus reality check. Exp. Dermatol. *20*, 697–702.

Kaur, P., Li, A., Redvers, R., and Bertoncello, I. (2004). Keratinocyte stem cell assays: an evolving science. J. Investig. Dermatol. Symp. Proc. *9*, 238–247.

Lim, X., Tan, S.H., Koh, W.L., Chau, R.M., Yan, K.S., Kuo, C.J., van Amerongen, R., Klein, A.M., and Nusse, R. (2013). Interfollicular epidermal stem cells self-renew via autocrine Wnt signaling. Science *342*, 1226–1230.

Liu, K., Jiang, M., Lu, Y., Chen, H., Sun, J., Wu, S., Ku, W.Y., Nakagawa, H., Kita, Y., Natsugoe, S., et al. (2013). Sox2 cooperates with inflammation-mediated Stat3 activation in the malignant transformation of foregut basal progenitor cells. Cell Stem Cell *12*, 304–315.

Lopez-Garcia, C., Klein, A.M., Simons, B.D., and Winton, D.J. (2010). Intestinal stem cell replacement follows a pattern of neutral drift. Science *330*, 822–825.

Marques-Pereira, J.P., and Leblond, C.P. (1965). Mitosis and differentiation in the stratified squamous epithelium of the rat esophagus. Am. J. Anat. *117*, 73–87.

Mascré, G., Dekoninck, S., Drogat, B., Youssef, K.K., Broheé, S., Sotiropoulou, P.A., Simons, B.D., and Blanpain, C. (2012). Distinct contribution of stem and progenitor cells to epidermal maintenance. Nature *489*, 257–262.

Maslov, A.Y., Barone, T.A., Plunkett, R.J., and Pruitt, S.C. (2004). Neural stem cell detection, characterization, and age-related changes in the subventricular zone of mice. J. Neurosci. *24*, 1726–1733.

Messier, B., and Leblond, C.P. (1960). Cell proliferation and migration as revealed by radioautography after injection of thymidine-H3 into male rats and mice. Am. J. Anat. *106*, 247–285.

Potten, C.S., and Loeffler, M. (1990). Stem cells: attributes, cycles, spirals, pitfalls and uncertainties. Lessons for and from the crypt. Development *110*, 1001–1020.

Que, J., Choi, M., Ziel, J.W., Klingensmith, J., and Hogan, B.L. (2006). Morphogenesis of the trachea and esophagus: current players and new roles for noggin and Bmps. Differentiation *74*, 422–437.

Ritsma, L., Ellenbroek, S.I., Zomer, A., Snippert, H.J., de Sauvage, F.J., Simons, B.D., Clevers, H., and van Rheenen, J. (2014). Intestinal crypt homeostasis revealed at single-stem-cell level by in vivo live imaging. Nature *507*, 362–365.

Sato, T., Vries, R.G., Snippert, H.J., van de Wetering, M., Barker, N., Stange, D.E., van Es, J.H., Abo, A., Kujala, P., Peters, P.J., and Clevers, H. (2009). Single Lgr5 stem cells build crypt-villus structures in vitro without a mesenchymal niche. Nature *459*, 262–265.

Sato, T., Stange, D.E., Ferrante, M., Vries, R.G., Van Es, J.H., Van den Brink, S., Van Houdt, W.J., Pronk, A., Van Gorp, J., Siersema, P.D., and Clevers, H. (2011). Long-term expansion of epithelial organoids from human colon, adenoma, adenocarcinoma, and Barrett's epithelium. Gastroenterology *141*, 1762–1772.

Seery, J.P. (2002). Stem cells of the oesophageal epithelium. J. Cell Sci. *115*, 1783–1789.

Snippert, H.J., van der Flier, L.G., Sato, T., van Es, J.H., van den Born, M., Kroon-Veenboer, C., Barker, N., Klein, A.M., van Rheenen, J., Simons, B.D., and Clevers, H. (2010). Intestinal crypt homeostasis results from neutral competition between symmetrically dividing Lgr5 stem cells. Cell *143*, 134–144.

Stingl, J., Eirew, P., Ricketson, I., Shackleton, M., Vaillant, F., Choi, D., Li, H.I., and Eaves, C.J. (2006). Purification and unique properties of mammary epithelial stem cells. Nature *439*, 993–997.

van der Flier, L.G., and Clevers, H. (2009). Stem cells, self-renewal, and differentiation in the intestinal epithelium. Annu. Rev. Physiol. *71*, 241–260.

Walther, V., and Graham, T.A. (2014). Location, location, location! The reality of life for an intestinal stem cell in the crypt. J. Pathol. *234*, 1–4.

Watt, F.M., and Hogan, B.L. (2000). Out of Eden: stem cells and their niches. Science *287*, 1427–1430.